

## Measurement of the $B_s$ Meson Lifetime

F. Abe,<sup>13</sup> M. G. Albrow,<sup>7</sup> S. R. Amendolia,<sup>23</sup> D. Amidei,<sup>16</sup> J. Antos,<sup>28</sup> C. Anway-Wiese,<sup>4</sup> G. Apollinari,<sup>26</sup> H. Areti,<sup>7</sup> M. Atac,<sup>7</sup> P. Auchincloss,<sup>25</sup> F. Azfar,<sup>21</sup> P. Azzi,<sup>20</sup> N. Bacchetta,<sup>18</sup> W. Badgett,<sup>16</sup> M. W. Bailey,<sup>18</sup> J. Bao,<sup>35</sup> P. de Barbaro,<sup>25</sup> A. Barbaro-Galtieri,<sup>14</sup> V. E. Barnes,<sup>24</sup> B. A. Barnett,<sup>12</sup> P. Bartalini,<sup>23</sup> G. Bauer,<sup>15</sup> T. Baumann,<sup>9</sup> F. Bedeschi,<sup>23</sup> S. Behrends,<sup>3</sup> S. Belforte,<sup>23</sup> G. Bellettini,<sup>23</sup> J. Bellinger,<sup>34</sup> D. Benjamin,<sup>31</sup> J. Benlloch,<sup>15</sup> J. Bensinger,<sup>3</sup> D. Benton,<sup>21</sup> A. Beretvas,<sup>7</sup> J. P. Berge,<sup>7</sup> S. Bertolucci,<sup>8</sup> A. Bhatti,<sup>26</sup> K. Biery,<sup>11</sup> M. Binkley,<sup>7</sup> F. Bird,<sup>29</sup> D. Bisello,<sup>20</sup> R. E. Blair,<sup>1</sup> C. Blocker,<sup>3</sup> A. Bodek,<sup>25</sup> W. Bokhari,<sup>15</sup> V. Bolognesi,<sup>23</sup> D. Bortoletto,<sup>24</sup> C. Boswell,<sup>12</sup> T. Boulos,<sup>14</sup> G. Brandenburg,<sup>9</sup> C. Bromberg,<sup>17</sup> E. Buckley-Geer,<sup>7</sup> H. S. Budd,<sup>25</sup> K. Burkett,<sup>16</sup> G. Busetto,<sup>20</sup> A. Byon-Wagner,<sup>7</sup> K. L. Byrum,<sup>1</sup> J. Cammerata,<sup>12</sup> C. Campagnari,<sup>7</sup> M. Campbell,<sup>16</sup> A. Caner,<sup>7</sup> W. Carithers,<sup>14</sup> D. Carlsmith,<sup>34</sup> A. Castro,<sup>20</sup> Y. Cen,<sup>21</sup> F. Cervelli,<sup>23</sup> H. Y. Chao,<sup>28</sup> J. Chapman,<sup>16</sup> M.-T. Cheng,<sup>28</sup> G. Chiarelli,<sup>8</sup> T. Chikamatsu,<sup>32</sup> C. N. Chiou,<sup>28</sup> S. Cihangir,<sup>7</sup> A. G. Clark,<sup>23</sup> M. Cobal,<sup>23</sup> M. Contreras,<sup>5</sup> J. Conway,<sup>27</sup> J. Cooper,<sup>7</sup> M. Cordelli,<sup>8</sup> C. Couyoumtzelis,<sup>23</sup> D. Crane,<sup>1</sup> J. D. Cunningham,<sup>3</sup> T. Daniels,<sup>15</sup> F. DeJongh,<sup>7</sup> S. Delchamps,<sup>7</sup> S. Dell'Agnello,<sup>23</sup> M. Dell'Orso,<sup>23</sup> L. Demortier,<sup>26</sup> B. Denby,<sup>23</sup> M. Deninno,<sup>2</sup> P. F. Derwent,<sup>16</sup> T. Devlin,<sup>27</sup> M. Dickson,<sup>25</sup> J. R. Dittmann,<sup>6</sup> S. Donati,<sup>23</sup> R. B. Drucker,<sup>14</sup> A. Dunn,<sup>16</sup> K. Einsweiler,<sup>14</sup> J. E. Elias,<sup>7</sup> R. Ely,<sup>14</sup> E. Engels, Jr.,<sup>22</sup> S. Eno,<sup>5</sup> D. Errede,<sup>10</sup> S. Errede,<sup>10</sup> Q. Fan,<sup>25</sup> B. Farhat,<sup>15</sup> I. Fiori,<sup>2</sup> B. Flaughner,<sup>7</sup> G. W. Foster,<sup>7</sup> M. Franklin,<sup>9</sup> M. Frautschi,<sup>18</sup> J. Freeman,<sup>7</sup> J. Friedman,<sup>15</sup> A. Fry,<sup>29</sup> T. A. Fuess,<sup>1</sup> Y. Fukui,<sup>13</sup> S. Funaki,<sup>32</sup> G. Gagliardi,<sup>23</sup> S. Galeotti,<sup>23</sup> M. Gallinaro,<sup>20</sup> A. F. Garfinkel,<sup>24</sup> S. Geer,<sup>7</sup> D. W. Gerdes,<sup>16</sup> P. Giannetti,<sup>23</sup> N. Giokaris,<sup>26</sup> P. Giromini,<sup>8</sup> L. Gladney,<sup>21</sup> D. Glenzinski,<sup>12</sup> M. Gold,<sup>18</sup> J. Gonzalez,<sup>21</sup> A. Gordon,<sup>9</sup> A. T. Goshaw,<sup>6</sup> K. Goulianos,<sup>26</sup> H. Grassmann,<sup>6</sup> A. Grewal,<sup>21</sup> G. Grieco,<sup>23</sup> L. Groer,<sup>27</sup> C. Grosso-Pilcher,<sup>5</sup> C. Haber,<sup>14</sup> S. R. Hahn,<sup>7</sup> R. Hamilton,<sup>9</sup> R. Handler,<sup>34</sup> R. M. Hans,<sup>35</sup> K. Hara,<sup>32</sup> B. Harral,<sup>21</sup> R. M. Harris,<sup>7</sup> S. A. Hauger,<sup>6</sup> J. Hauser,<sup>4</sup> C. Hawk,<sup>27</sup> J. Heinrich,<sup>21</sup> D. Cronin-Hennessy,<sup>6</sup> R. Hollebeek,<sup>21</sup> L. Holloway,<sup>10</sup> A. Hölcher,<sup>11</sup> S. Hong,<sup>16</sup> G. Houk,<sup>21</sup> P. Hu,<sup>22</sup> B. T. Huffman,<sup>22</sup> R. Hughes,<sup>25</sup> P. Hurst,<sup>9</sup> J. Huston,<sup>17</sup> J. Huth,<sup>9</sup> J. Huyen,<sup>7</sup> M. Incagli,<sup>23</sup> J. Incandela,<sup>7</sup> H. Iso,<sup>32</sup> H. Jensen,<sup>7</sup> C. P. Jessop,<sup>9</sup> U. Joshi,<sup>7</sup> R. W. Kadel,<sup>14</sup> E. Kajfasz,<sup>7,\*</sup> T. Kamon,<sup>30</sup> T. Kaneko,<sup>32</sup> D. A. Kardelis,<sup>10</sup> H. Kasha,<sup>35</sup> Y. Kato,<sup>19</sup> L. Keeble,<sup>8</sup> R. D. Kennedy,<sup>27</sup> R. Kephart,<sup>7</sup> P. Kesten,<sup>14</sup> D. Kestenbaum,<sup>9</sup> R. M. Keup,<sup>10</sup> H. Keutelian,<sup>7</sup> F. Keyvan,<sup>4</sup> D. H. Kim,<sup>7</sup> H. S. Kim,<sup>11</sup> S. B. Kim,<sup>16</sup> S. H. Kim,<sup>32</sup> Y. K. Kim,<sup>14</sup> L. Kirsch,<sup>3</sup> P. Koehn,<sup>25</sup> K. Kondo,<sup>32</sup> J. Konigsberg,<sup>9</sup> S. Kopp,<sup>5</sup> K. Kordas,<sup>11</sup> W. Koska,<sup>7</sup> E. Kovacs,<sup>7,\*</sup> W. Kowald,<sup>6</sup> M. Krasberg,<sup>16</sup> J. Kroll,<sup>7</sup> M. Kruse,<sup>24</sup> S. E. Kuhlmann,<sup>1</sup> E. Kuns,<sup>27</sup> A. T. Laasanen,<sup>24</sup> N. Labanca,<sup>23</sup> S. Lammell,<sup>4</sup> J. I. Lamoureux,<sup>3</sup> T. LeCompte,<sup>10</sup> S. Leone,<sup>23</sup> J. D. Lewis,<sup>7</sup> P. Limon,<sup>7</sup> M. Lindgren,<sup>4</sup> T. M. Liss,<sup>10</sup> N. Lockyer,<sup>21</sup> C. Loomis,<sup>27</sup> O. Long,<sup>21</sup> M. Loretì,<sup>20</sup> E. H. Low,<sup>21</sup> J. Lu,<sup>30</sup> D. Lucchesi,<sup>23</sup> C. B. Luchini,<sup>10</sup> P. Lukens,<sup>7</sup> P. Maas,<sup>34</sup> K. Maeshima,<sup>7</sup> A. Maghakian,<sup>26</sup> P. Maksimovic,<sup>15</sup> M. Mangano,<sup>23</sup> J. Mansour,<sup>17</sup> M. Mariotti,<sup>23</sup> J. P. Marriner,<sup>7</sup> A. Martin,<sup>10</sup> J. A. J. Matthews,<sup>18</sup> R. Mattingly,<sup>15</sup> P. McIntyre,<sup>30</sup> P. Melese,<sup>26</sup> A. Menzione,<sup>23</sup> E. Meschi,<sup>23</sup> G. Michail,<sup>9</sup> S. Mikamo,<sup>13</sup> M. Miller,<sup>5</sup> R. Miller,<sup>17</sup> T. Mimashi,<sup>32</sup> S. Miscetti,<sup>8</sup> M. Mishina,<sup>13</sup> H. Mitsushio,<sup>32</sup> S. Miyashita,<sup>32</sup> Y. Morita,<sup>13</sup> S. Moulding,<sup>26</sup> J. Mueller,<sup>27</sup> A. Mukherjee,<sup>7</sup> T. Muller,<sup>4</sup> P. Musgrave,<sup>11</sup> L. F. Nakae,<sup>29</sup> I. Nakano,<sup>32</sup> C. Nelson,<sup>7</sup> D. Neuberger,<sup>4</sup> C. Newman-Holmes,<sup>7</sup> L. Nodulman,<sup>1</sup> S. Ogawa,<sup>32</sup> S. H. Oh,<sup>6</sup> K. E. Ohl,<sup>35</sup> R. Oishi,<sup>32</sup> T. Okusawa,<sup>19</sup> C. Pagliarone,<sup>23</sup> R. Paoletti,<sup>23</sup> V. Papadimitriou,<sup>31</sup> S. Park,<sup>7</sup> J. Patrick,<sup>7</sup> G. Pauletta,<sup>23</sup> M. Paulini,<sup>14</sup> L. Pescara,<sup>20</sup> M. D. Peters,<sup>14</sup> T. J. Phillips,<sup>6</sup> G. Piacentino,<sup>2</sup> M. Pillai,<sup>25</sup> R. Plunkett,<sup>7</sup> L. Pondrom,<sup>34</sup> N. Produit,<sup>14</sup> J. Proudfoot,<sup>1</sup> F. Ptohos,<sup>9</sup> G. Punzi,<sup>23</sup> K. Ragan,<sup>11</sup> F. Rimondi,<sup>2</sup> L. Ristori,<sup>23</sup> M. Roach-Bellino,<sup>33</sup> W. J. Robertson,<sup>6</sup> T. Rodrigo,<sup>7</sup> J. Romano,<sup>5</sup> L. Rosenson,<sup>15</sup> W. K. Sakumoto,<sup>25</sup> D. Saltzberg,<sup>5</sup> A. Sansoni,<sup>8</sup> V. Scarpine,<sup>30</sup> A. Schindler,<sup>14</sup> P. Schlabach,<sup>9</sup> E. E. Schmidt,<sup>7</sup> M. P. Schmidt,<sup>35</sup> O. Schneider,<sup>14</sup> G. F. Sciacca,<sup>23</sup> A. Scribano,<sup>23</sup> S. Segler,<sup>7</sup> S. Seidel,<sup>18</sup> Y. Seiya,<sup>32</sup> G. Sganos,<sup>11</sup> A. Sgolacchia,<sup>2</sup> M. Shapiro,<sup>14</sup> N. M. Shaw,<sup>24</sup> Q. Shen,<sup>24</sup> P. F. Shepard,<sup>22</sup> M. Shimojima,<sup>32</sup> M. Shochet,<sup>5</sup> J. Siegrist,<sup>29</sup> A. Sill,<sup>31</sup> P. Sinervo,<sup>11</sup> P. Singh,<sup>22</sup> J. Skarha,<sup>12</sup> K. Sliwa,<sup>33</sup> D. A. Smith,<sup>23</sup> F. D. Snider,<sup>12</sup> L. Song,<sup>7</sup> T. Song,<sup>16</sup> J. Spalding,<sup>7</sup> L. Spiegel,<sup>7</sup> P. Sphicas,<sup>15</sup> A. Spies,<sup>12</sup> L. Stanco,<sup>20</sup> J. Steele,<sup>34</sup> A. Stefanini,<sup>23</sup> K. Strahl,<sup>11</sup> J. Strait,<sup>7</sup> D. Stuart,<sup>7</sup> G. Sullivan,<sup>5</sup> K. Sumorok,<sup>15</sup> R. L. Swartz, Jr.,<sup>10</sup> T. Takahashi,<sup>19</sup> K. Takikawa,<sup>32</sup> F. Tartarelli,<sup>23</sup> W. Taylor,<sup>11</sup> P. K. Teng,<sup>28</sup> Y. Teramoto,<sup>19</sup> S. Tether,<sup>15</sup> D. Theriot,<sup>7</sup> J. Thomas,<sup>29</sup> T. L. Thomas,<sup>18</sup> R. Thun,<sup>16</sup> M. Timko,<sup>33</sup> P. Tipton,<sup>25</sup> A. Titov,<sup>26</sup> S. Tkaczyk,<sup>7</sup> K. Tollefson,<sup>25</sup> A. Tollestrup,<sup>7</sup> J. Tonnison,<sup>24</sup> J. F. de Troconiz,<sup>9</sup> J. Tseng,<sup>12</sup> M. Turcotte,<sup>29</sup> N. Turini,<sup>2</sup> N. Uemura,<sup>32</sup> F. Ukegawa,<sup>21</sup> G. Unal,<sup>21</sup> S. van den Brink,<sup>22</sup> S. Vejcik III,<sup>16</sup> R. Vidal,<sup>7</sup> M. Vondracek,<sup>10</sup> R. G. Wagner,<sup>1</sup> R. L. Wagner,<sup>7</sup> N. Wainer,<sup>7</sup> R. C. Walker,<sup>25</sup> C. H. Wang,<sup>28</sup> G. Wang,<sup>23</sup> J. Wang,<sup>5</sup> M. J. Wang,<sup>28</sup> Q. F. Wang,<sup>26</sup> A. Warburton,<sup>11</sup> G. Watts,<sup>25</sup> T. Watts,<sup>27</sup> R. Webb,<sup>30</sup> C. Wendt,<sup>34</sup> H. Wenzel,<sup>14</sup> W. C. Wester III,<sup>14</sup> T. Westhusing,<sup>10</sup> A. B. Wicklund,<sup>1</sup> E. Wicklund,<sup>7</sup> R. Wilkinson,<sup>21</sup> H. H. Williams,<sup>21</sup> P. Wilson,<sup>5</sup> B. L. Winer,<sup>25</sup> J. Wolinski,<sup>30</sup> D. Y. Wu,<sup>16</sup> X. Wu,<sup>23</sup> J. Wyss,<sup>20</sup> A. Yagil,<sup>7</sup> W. Yao,<sup>14</sup> K. Yasuoka,<sup>32</sup> Y. Ye,<sup>11</sup>

G. P. Yeh,<sup>7</sup> P. Yeh,<sup>28</sup> M. Yin,<sup>6</sup> J. Yoh,<sup>7</sup> T. Yoshida,<sup>19</sup> D. Yovanovitch,<sup>7</sup> I. Yu,<sup>35</sup> J. C. Yun,<sup>7</sup> A. Zanetti,<sup>23</sup> F. Zetti,<sup>23</sup>  
L. Zhang,<sup>34</sup> S. Zhang,<sup>16</sup> W. Zhang,<sup>21</sup> and S. Zucchelli<sup>2</sup>

(CDF Collaboration)

<sup>1</sup>Argonne National Laboratory, Argonne, Illinois 60439

<sup>2</sup>Istituto Nazionale di Fisica Nucleare, University of Bologna, I-40126 Bologna, Italy

<sup>3</sup>Brandeis University, Waltham, Massachusetts 02254

<sup>4</sup>University of California at Los Angeles, Los Angeles, California 90024

<sup>5</sup>University of Chicago, Chicago, Illinois 60637

<sup>6</sup>Duke University, Durham, North Carolina 27708

<sup>7</sup>Fermi National Accelerator Laboratory, Batavia, Illinois 60510

<sup>8</sup>Laboratori Nazionali di Frascati, Istituto Nazionale di Fisica Nucleare, I-00044 Frascati, Italy

<sup>9</sup>Harvard University, Cambridge, Massachusetts 02138

<sup>10</sup>University of Illinois, Urbana, Illinois 61801

<sup>11</sup>Institute of Particle Physics, McGill University, Montreal, Canada H3A 2T8  
and University of Toronto, Toronto, Canada M5S 1A7

<sup>12</sup>The Johns Hopkins University, Baltimore, Maryland 21218

<sup>13</sup>National Laboratory for High Energy Physics (KEK), Tsukuba, Ibaraki 305, Japan

<sup>14</sup>Lawrence Berkeley Laboratory, Berkeley, California 94720

<sup>15</sup>Massachusetts Institute of Technology, Cambridge, Massachusetts 02139

<sup>16</sup>University of Michigan, Ann Arbor, Michigan 48109

<sup>17</sup>Michigan State University, East Lansing, Michigan 48824

<sup>18</sup>University of New Mexico, Albuquerque, New Mexico 87131

<sup>19</sup>Osaka City University, Osaka 588, Japan

<sup>20</sup>Università di Padova, Istituto Nazionale di Fisica Nucleare, Sezione di Padova, I-35131 Padova, Italy

<sup>21</sup>University of Pennsylvania, Philadelphia, Pennsylvania 19104

<sup>22</sup>University of Pittsburgh, Pittsburgh, Pennsylvania 15260

<sup>23</sup>Istituto Nazionale di Fisica Nucleare, University and Scuola Normale Superiore of Pisa, I-56100 Pisa, Italy

<sup>24</sup>Purdue University, West Lafayette, Indiana 47907

<sup>25</sup>University of Rochester, Rochester, New York 14627

<sup>26</sup>Rockefeller University, New York, New York 10021

<sup>27</sup>Rutgers University, Piscataway, New Jersey 08854

<sup>28</sup>Accademia Sinica, Taiwan 11529, Republic of China

<sup>29</sup>Superconducting Super Collider Laboratory, Dallas, Texas 75237

<sup>30</sup>Texas A&M University, College Station, Texas 77843

<sup>31</sup>Texas Tech University, Lubbock, Texas 79409

<sup>32</sup>University of Tsukuba, Tsukuba, Ibaraki 305, Japan

<sup>33</sup>Tufts University, Medford, Massachusetts 02155

<sup>34</sup>University of Wisconsin, Madison, Wisconsin 53706

<sup>35</sup>Yale University, New Haven, Connecticut 06511

(Received 22 December 1994)

The lifetime of the  $B_s$  meson is measured using the semileptonic decay  $B_s \rightarrow D_s^- \ell^+ \nu X$ . The data sample consists of  $19.3 \text{ pb}^{-1}$  of  $p\bar{p}$  collisions at  $\sqrt{s} = 1.8 \text{ TeV}$  collected by the Collider Detector at Fermilab during 1992–1993. There are  $76 \pm 8 \ell^+ D_s^-$  signal events where the  $D_s$  is identified via the decay  $D_s^- \rightarrow \phi \pi^-$ ,  $\phi \rightarrow K^+ K^-$ . Using these events, the  $B_s$  meson lifetime is determined to be  $\tau_s = 1.42^{+0.27}_{-0.23}(\text{stat}) \pm 0.11(\text{syst}) \text{ ps}$ . A measurement of the  $B_s$  lifetime in a low statistics sample of exclusive  $B_s \rightarrow J/\psi \phi$  decays is also presented in this paper.

PACS numbers: 13.25.Hw, 14.40.Nd

The lifetime differences between the bottom hadrons can probe the  $B$ -decay mechanisms which are beyond the simple quark spectator model. In the case of charm mesons, such differences have been observed to be quite large [ $\tau(D^+)/\tau(D^0) \sim 2.5$ ]. Among bottom hadrons, the lifetime differences are expected to be smaller due to the heavier bottom quark mass. Phenomenological models predict a (5–10)% difference between the  $B_u$  and  $B_d$  meson lifetimes and very similar  $B_d$  and  $B_s$  lifetimes [1]. This is consistent with the previous measurements

of  $B_{u,d}$  meson lifetime [2] as well as recent  $B_s$  lifetime measurements from the CERN  $e^+e^-$  collider LEP [3]. It has also been suggested by recent theory calculations [4] that the lifetime between the two  $CP$  eigenstates produced by mixing of the  $B_s$  and  $\bar{B}_s$  may differ by as much as 15%. Such an effect may manifest itself as a difference in lifetimes between the  $B_s$  semileptonic decay, which is almost an equal mixture of the two  $CP$  states, and the decay  $B_s \rightarrow J/\psi \phi$ , which is expected to be dominated by the  $CP$  even state. In this Letter, we first present

the measurement of  $B_s$  lifetime using the semileptonic decay [5]  $B_s \rightarrow D_s^- \ell^+ \nu X$ , where the  $D_s^-$  is identified via  $D_s^- \rightarrow \phi \pi^-$ ,  $\phi \rightarrow K^+ K^-$ . We then describe briefly a result using the exclusive decay  $B_s \rightarrow J/\psi \phi$ , where  $J/\psi \rightarrow \mu^+ \mu^-$ ,  $\phi \rightarrow K^+ K^-$ . The data sample for this paper consists of  $19.3 \text{ pb}^{-1}$  of  $p\bar{p}$  collisions at  $\sqrt{s} = 1.8 \text{ TeV}$  collected by the Collider Detector at Fermilab (CDF) during the 1992–1993 run.

The CDF is described in detail elsewhere [6]. We describe here only the detector features most relevant to this analysis. Two devices inside the 1.4 T solenoid are used for the tracking of charged particles: the silicon vertex detector (SVX) and the central tracking chamber (CTC). The SVX consists of four layers of silicon microstrip detectors and provides spatial measurements in the  $r$ - $\phi$  plane [7], giving a track impact parameter resolution of about  $(13 + 40/p_T) \mu\text{m}$  [8], where  $p_T$  is the transverse momentum of the track in  $\text{GeV}/c$ . The transverse profile of the beam is circular and has an rms of  $\sim 35 \mu\text{m}$ , while the longitudinal beam size is  $\sim 30 \text{ cm}$ . The CTC is a cylindrical drift chamber containing 84 layers grouped into eight alternating superlayers of axial and stereo wires. It covers the pseudorapidity interval  $|\eta| < 1.1$ , where  $\eta = -\ln[\tan(\theta/2)]$ . Outside the solenoid are electromagnetic (CEM) and hadronic (CHA) calorimeters ( $|\eta| < 1.1$ ) that employ a projective tower geometry. A layer of proportional wire chambers (CES) is located near shower maximum in the CEM and provides a measurement of electromagnetic shower profiles in both the  $\phi$  and  $z$  directions. Two muon subsystems in the central region are used, the central muon chambers (CMU) and the central upgrade muon chambers (CMP), with total coverage of 80% for  $|\eta| \leq 0.6$ . The CMP chambers are located behind eight interaction lengths of material.

Events containing semileptonic  $B_s$  decays were collected using inclusive electron and muon triggers. The  $E_T$  threshold for the principal single electron trigger was 9 GeV, where  $E_T \equiv E \sin(\theta)$  and  $E$  is the electromagnetic energy measured in the calorimeter. The single muon trigger required a  $p_T > 7.5 \text{ GeV}/c$  track in the CTC with matched track segments in both the CMU and CMP systems. Off-line identification of an electron and muon was described in Refs. [9] and [10].

The  $D_s^- \rightarrow \phi \pi^-$  reconstruction started with a search for  $\phi$  candidates. We first defined a search cone around the lepton candidate with a radius  $\Delta R = \sqrt{(\Delta\eta)^2 + (\Delta\phi)^2}$  of 0.8. Any two oppositely charged tracks with  $p_T > 1 \text{ GeV}/c$  within that cone were assigned kaon masses and combined to form a  $\phi$  candidate. Each  $\phi$  candidate was required to have  $p_T(\phi) > 2.0 \text{ GeV}/c$  and a mass within  $\pm 8 \text{ MeV}/c^2$  of the world average  $\phi$  mass [11]. The  $\phi$  candidate was then combined with another track of  $p_T > 0.8 \text{ GeV}/c$  inside the cone which had the opposite charge of the lepton (the “right-sign” combination). This third track was assigned the pion mass. To ensure a good decay vertex measurement, track quality cuts were imposed on

the lepton and at least two of the three track candidates formed the  $D_s$  candidate. The  $K^+$ ,  $K^-$ , and  $\pi^-$  tracks were then fit with a common vertex constraint, and the confidence level was required to be  $> 1\%$ . Since the  $\phi$  has spin 1 and both the  $D_s^-$  and  $\pi^-$  are spin 0, the helicity angle  $\Psi$ , which is the angle between the  $K^+$  and  $D_s^-$  directions in the  $\phi$  rest frame, exhibits a distribution  $dN/d(\cos\Psi) \sim \cos^2\Psi$ . A cut  $|\cos\Psi| > 0.4$  was therefore applied to suppress the combinatorial background, which we found to be a flat distribution in  $\cos\Psi$ . The mass of the  $\ell D_s$  system was required to be between 3.0 and 5.7  $\text{GeV}/c^2$  in order to be consistent with coming from a  $B_s$  decay. We also applied an isolation cut  $E_T^{\text{iso}}/p_T(\phi\pi^-) < 1.2$  on the  $D_s^-$  candidate, where  $E_T^{\text{iso}}$  is a sum of transverse energy within a cone of radius 0.4 in  $\eta$ - $\phi$  space around the lepton candidate, excluding the lepton energy. This cut eliminated many of the fake  $D_s^-$  combinations from high track multiplicity jets. Furthermore, we required that the apparent  $D_s^-$  decay vertex ( $V_D$ ) be positively displaced from the primary vertex along the direction of the  $\ell^+ D_s^-$  momentum. Figure 1(a) shows the  $\phi\pi^-$  invariant mass distribution for the right-sign lepton- $D_s$  combinations. A  $D_s$  signal with mean of 1.967  $\text{GeV}/c^2$  and width of 5.4  $\text{MeV}/c^2$  is observed. Evidence of the Cabibbo suppressed  $D^- \rightarrow \phi\pi^-$  decay is also present. No enhancement is seen in the corresponding distribution for the “wrong-sign” combinations [Fig. 1(b)]. (Because of stringent lepton selection criteria, events with a fake lepton accompanied by a  $D_s$  are expected to be rare.) We select a signal sample using a  $D_s^-$  mass window of 1.953 to 1.981  $\text{GeV}/c^2$ . The number of  $\ell^+ D_s^-$  events above background in the sample is  $76 \pm 8$  out of a total of 139 events.

There are two possible sources of nonstrange  $B$  meson decays which can lead to right-sign  $\ell^+ D_s^-$  combinations.

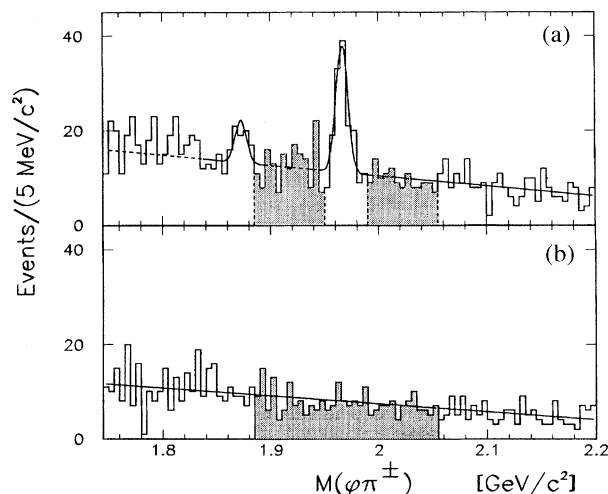


FIG. 1. The mass distribution of  $\phi\pi^-$  for (a) “right-sign” combination ( $\phi\pi^-\ell^+$ ); (b) “wrong-sign” combination ( $\phi\pi^-\ell^-$ ). The shaded regions are used for the background sample.

The four-body decay  $B_{u,d} \rightarrow D_s^- \mathcal{K} \ell^+ \nu$ , where  $\mathcal{K}$  denotes any type of strange meson, has not been observed experimentally [12]. Based on the theoretical limit  $\mathcal{B}(B_{u,d} \rightarrow D_s^- \mathcal{K} \ell^+ \nu) \leq 0.025 \mathcal{B}(B_d \rightarrow \ell^+ \nu X)$  [13], we expect less than 2.6% of our  $\ell^+ D_s^-$  combinations from this source. The second process is  $\bar{B}_{u,d} \rightarrow D_s^- DX, D \rightarrow \ell^+ \nu X$ , where  $D$  is any charmed meson. This decay produces softer and less isolated leptons than that from  $B_s$  semileptonic decay. Using the  $\mathcal{B}(B \rightarrow D_s X)$  [14,15] and the semileptonic branching ratios of  $D^0$  and  $D^+$  [11], we estimate the fraction of this type of background is less than 3%. In addition, we also considered the background from  $c\bar{c}$  production where a  $D_s^- D$  pair is produced. Monte Carlo simulation predicts the background fraction from this type of source to be  $<7\%$ . In summary, the contribution of all above physics backgrounds is small, and we consider them as a source of systematic uncertainty.

The secondary vertex where the  $B_s$  decays to a lepton and a  $D_s^-$  (referred to as  $V_{B_s}$ ) is obtained in the transverse plane by intersecting the trajectory of the lepton track with the flight path of the  $D_s^-$  candidate. The transverse decay length  $L$  is defined as the displacement in the transverse plane of  $V_{B_s}$  from the primary vertex projected onto the direction of the  $p_T(\ell D_s)$ . The effect of the relativistic boost can be partially removed event by event with the factor  $p_T(\ell D_s)/M(B_s)$  [where  $M(B_s) = 5.37 \text{ GeV}/c^2$  [16]] and leads to a corrected decay length  $\xi = LM(B_s)/p_T(\ell D_s)$  which is referred to as the ‘‘proper decay length.’’ A residual correction between  $p_T(\ell D_s)$  and  $p_T(B_s)$  is done statistically by convoluting a Monte Carlo distribution of the  $p_T$  correction factor  $\mathcal{K} = p_T(\ell D_s)/p_T(B_s)$  with an exponential decay distribution in the lifetime fit. The  $\mathcal{K}$  distribution has an average value of 0.86 and an rms of 0.11 and is approximately constant as a function of  $p_T(\ell D_s)$ . To model the proper decay length distribution of the background events contained in the signal sample, we define a background sample which consists of the right-sign events from the  $D_s^-$  sidebands (1.885–1.945 and 1.990–2.050  $\text{GeV}/c^2$ ) and the wrong-sign events from the interval 1.885–2.050  $\text{GeV}/c^2$ .

The proper decay length distribution (Fig. 2) is fit using an unbinned maximum log-likelihood method. Both the  $B_s$  lifetime and the background shape are determined in a simultaneous fit using the signal and background samples. Thus the likelihood function  $\mathcal{L}$  is a combination of two parts:  $\mathcal{L} = \prod_i^{N_S} [(1 - f_{bg}) \mathcal{F}_{Sig}^i + f_{bg} \mathcal{F}_{bg}^i] \cdot \prod_j^{N_B} \mathcal{F}_{bg}^j$ , where  $N_S$  and  $N_B$  are the number of events in the signal and background samples. The signal probability function  $\mathcal{F}_{Sig}$  consists of a normalized decay exponential function (defined for only positive decay lengths) convoluted with the  $\mathcal{K}$  distribution and a Gaussian resolution function where an event-by-event based decay length uncertainty (typically 100  $\mu\text{m}$ ) is used. A scale factor  $s$  is introduced to account for the underestimation of the decay length un-

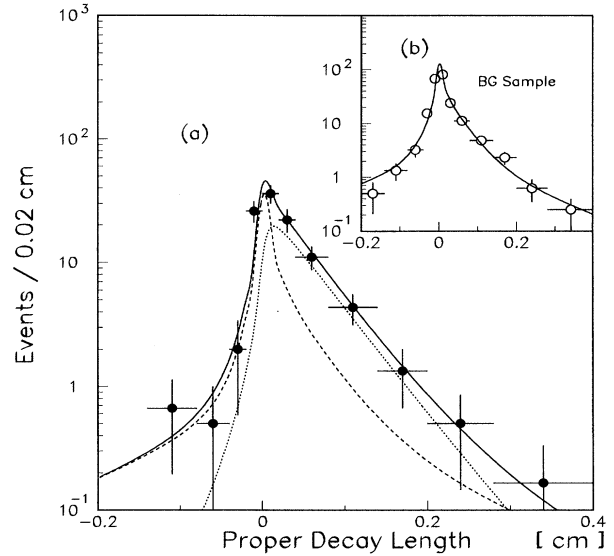


FIG. 2. Proper decay length distribution (a) for the  $\ell^+ D_s^-$  signal sample with a curve (solid) from an unbinned log-likelihood fitting of signal (dotted) and background (dashed) and (b) for the background sample with a fitting curve.

certainty. The background is parametrized by a Gaussian centered at zero, symmetrical positive and negative exponential tails, and a positive decay exponential to characterize the heavy flavor decay in the background sample. The best fit values of  $c\tau$  and  $s$  are found to be  $426_{-68}^{+80} \mu\text{m}$  and  $1.4 \pm 0.1$ , respectively. Figure 2(a) shows the proper decay length distribution of the signal sample with the result of the fit superimposed. The same distribution of the background samples is shown in Fig. 2(b). As a consistency check, we fit the  $D_s$  lifetime from the proper decay length measured from the tertiary vertex  $V_{D_s}$  to the secondary vertex  $V_{B_s}$ . The result is  $c\tau_{D_s} = 135_{-30}^{+40} \mu\text{m}$ , which is consistent with the world average value [11].

All sources of systematic uncertainty are studied. Major contributions come from the source of the background shape, the non- $B_s$  production, and the resolution function. Three regions of sideband were used to determine the background shape. We find a  $\pm 4\%$  variation in the lifetime result when using each sideband region individually. The dominant source of systematics from non- $B_s$  production was found to be  $\bar{B}_{u,d} \rightarrow D_s^- DX$  decays. This mode was studied using Monte Carlo simulations and the contribution to the systematic uncertainty in the lifetime was found to be  $\pm 4\%$ . The effect of the decay length resolution was studied by varying the scale factor and using an alternative resolution function consisting of two Gaussians, giving a 3% systematic uncertainty. The rest of the contributions include relativistic boost correction 2%, decay length cut 2%, fitting method 1%, and misalignment 2%. The overall systematic uncertainty is 7%.

Quoting the statistical and systematic uncertainties separately, we measure the  $B_s$  lifetime using semileptonic decays to be  $\tau_{B_s} = 1.42^{+0.27}_{-0.23}(\text{stat}) \pm 0.11(\text{syst})$  ps. This result is consistent with the previous world average of  $1.34^{+0.32}_{-0.27}$  ps [11].

For the exclusive mode measurement, we use the decay chain  $B_s \rightarrow J/\psi \phi$ ,  $J/\psi \rightarrow \mu^+ \mu^-$ ,  $\phi \rightarrow K^+ K^-$ . The data sample and reconstruction techniques used for this decay channel are similar to those described in detail elsewhere [17]. Briefly, the invariant mass of two oppositely charged muon candidates is calculated after the tracks are constrained to originate from a common vertex.  $J/\psi$  candidates are selected by requiring the difference between the dimuon mass and the world average  $J/\psi$  mass [11] to be  $< 3\sigma$ , where  $\sigma$  is the mass uncertainty calculated for each dimuon candidate. The  $\phi$  meson selections are the same as Ref. [17] but with  $p_T(\phi) > 3.0$  (rather than 2 GeV/c) to further reduce the background.

Using the measured  $p_T(B_s)$ , the proper decay length is calculated and the lifetime of the  $B_s$  meson is determined by performing a simultaneous unbinned log-likelihood fit to the entire mass and proper decay length spectra. The mass distribution is fit to a Gaussian and a flat background. We model the proper decay length distribution of the background with a Gaussian centered at zero and positive and negative exponential functions. The signal is described by an exponential decay function convoluted with a Gaussian. This fit determines the mass and lifetime of the  $B_s$ , the signal fraction, and background shape simultaneously. The proper decay length distribution is shown in Fig. 3, where we have displayed events within

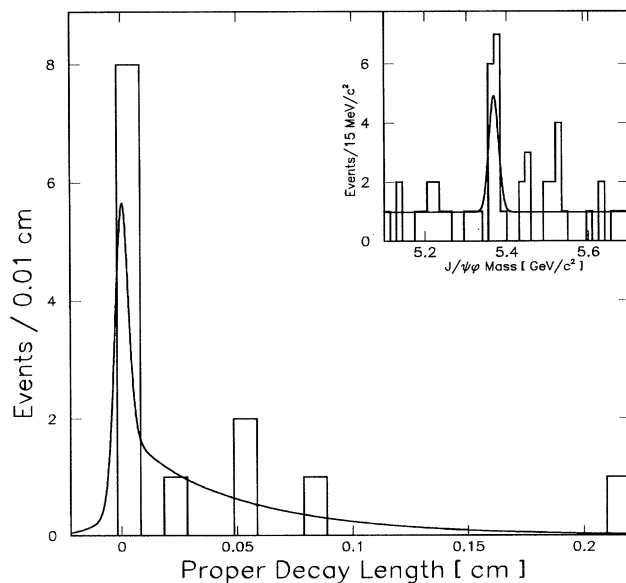


FIG. 3.  $B_s$  lifetime measurement using the  $J/\psi \phi$  exclusive mode. Inset figure is the mass distribution. The solid curves show the fit results.

$\pm 21$  MeV/c<sup>2</sup> of the  $B_s$  mass peak. The  $B_s$  lifetime was found to be  $1.74^{+1.08}_{-0.69}(\text{stat}) \pm 0.07(\text{syst})$  ps with  $7.9^{+3.6}_{-1.6}$  signal events. The dominant systematic error ( $\pm 20 \mu\text{m}$ ) arises from the uncertainty in the parametrization of the background shape and the resolution function.

In conclusion, the  $B_s$  lifetime has been measured for the first time in a hadronic environment. The semileptonic and exclusive results are consistent with each other at present. They are also consistent with the results of the  $B_u$  and  $B_d$  lifetimes previously measured by CDF. We anticipate a more significant result in both modes after the ongoing collider run.

We thank the Fermilab staff and the technical staffs of the participating institutions for their vital contributions. This work was supported by the U.S. Department of Energy and National Science Foundation, the Italian Istituto Nazionale di Fisica Nucleare, the Ministry of Education, Science and Culture of Japan, the Natural Sciences and Engineering Research Council of Canada, the National Science Council of the Republic of China, the A. P. Sloan Foundation, and the Alexander von Humboldt-Stiftung.

\*Visitor.

- [1] M. B. Voloshin and M. A. Shifman, Sov. Phys. JETP **64**, 698 (1986).
- [2] F. Abe *et al.*, Phys. Rev. Lett. **72**, 3456 (1994); S. Wagner *et al.*, *ibid.* **64**, 1095 (1990); P. Abreu *et al.*, Z. Phys. C **57**, 181 (1993); D. Buskulic *et al.*, Phys. Lett. B **297**, 449 (1992); D. Buskulic *et al.*, *ibid.* **307**, 194 (1993); D. Buskulic *et al.*, *ibid.* **314**, 459 (1993); P. D. Acton *et al.*, *ibid.* **307**, 247 (1993).
- [3] P. D. Acton *et al.*, Phys. Lett. B **312**, 501 (1993); P. Abreu *et al.*, Z. Phys. C **61**, 407 (1994); D. Buskulic *et al.*, Phys. Lett. B **322**, 275 (1994).
- [4] I. I. Bigi *et al.*, CERN Report No. CERN-TH.7132/94; R. Aleksan *et al.*, Phys. Lett. B **316**, 567 (1993).
- [5] References to a specific charge state imply the charge-conjugate state as well.
- [6] F. Abe *et al.*, Nucl. Instrum. Methods Phys. Res., Sect. A **271**, 387 (1988).
- [7] In CDF,  $\varphi$  is the azimuthal angle,  $\theta$  is the polar angle measured from the proton direction, and  $r$  is the radius from the beam axis ( $z$  axis).
- [8] D. Amidei *et al.*, Nucl. Instrum. Methods Phys. Res., Sect. A **350**, 73 (1994).
- [9] F. Abe *et al.*, Phys. Rev. Lett. **71**, 500 (1993).
- [10] F. Abe *et al.*, Phys. Rev. Lett. **71**, 3421 (1993).
- [11] Particle Data Group, L. Montanet *et al.*, Phys. Rev. D **50**, 1173 (1994).
- [12] H. Albrecht *et al.*, Z. Phys. C **60**, 11 (1993).
- [13] E. Golowich *et al.*, Z. Phys. C **48**, 89 (1990).
- [14] D. Bortoletto *et al.*, Phys. Rev. Lett. **64**, 2117 (1990).
- [15] H. Albrecht *et al.*, Z. Phys. C **54**, 1 (1992).
- [16] Y. Cen, Ph.D. thesis, University of Pennsylvania, 1994.
- [17] F. Abe *et al.*, Phys. Rev. Lett. **71**, 1685 (1993).